A R C H I V E S O F M E T A L L U R G Y A N D M A T E R I A L S
Volume 52 2007 Issue 4

A. PAWŁOWSKI *, J. MORGIEL *, T. CZEPPE *

AMORPHISATION AND CRYSTALLISATION OF PHASES IN PLASMA SPRAYED Al_2O_3 AND ZrO_2 BASED CERAMICS

AMORFIZACJA I KRYSTALIZACJA FAZ W CERAMICE NA BAZIE Al_2O_3 i ZrO_2 NATRYSKIWANEJ PLAZMOWO

The susceptibility to glass formation in the group of four Al_2O_3-SiO_2, Al_2O_3-TiO_2, Al_2O_3-ZrO_2 and ZrO_2-Y_2O_3 ceramics alloys plasma sprayed on a metallic substrate, commonly used for thermal shields of diesel engine parts, were studied in the work. In the ceramic layers produced in such a way an amorphous sublayer solidified on a surface of the substrate. The layers were analysed using techniques of electron microscopy (SADP and EDX). It was established, that although all studied alloys revealed amorphous sublayers, the Al_2O_3-SiO_2 materials were more prone to glass formation than the ZrO_2-Y_2O_3 ones. An annealing of the amorphous layers resulted in their partial crystallisation.
Keywords: thermal barier coatings, plasma spraying, phase transitions

W pracy analizowano podatność na zeszklenie grupy materiałów ceramicznych typu Al_2O_3-SiO_2, Al_2O_3-TiO_2, Al_2O_3-ZrO_2 oraz ZrO_2-Y_2O_3, natryskiwanych plazmowo na podłoże metaliczne, stosowanych na bariery termiczne części silników wysokoprężnych. W tak otrzymanych warstwach ceramicznych można wyodrębnić podwarstwę o budowie amorficznej, na granicy z podłożem. Uzyskane warstwy analizowano technikami mikroskopii elektronowej (SADP oraz EDX). Wykazano, że wspomniane podwarstwy charakteryzowały się budową amorficzną we wszystkich analizowanych stopach ceramicznych, jednak największą podatność do amorfizacji wykazały tworzywa Al_2O_3-SiO_2, zaś najmniejszą ZrO_2-Y_2O_3. Wyżarzanie faz amorficznych o tym składzie powodowało częściową ich krystalizację.

1. Introduction

The plasma sprayed oxide materials of the type: (1) Al_2O_3-30 wt.% SiO_2; (2) Al_2O_3-40 wt.% TiO_2; (3) Al_2O_3-40 wt.% ZrO_2; (4) ZrO_2-20 wt.% Y_2O_3 show composite morphology of the sublayer of low thermal conductivity and high temperature of performance. Such thermal barriers shield from heat the steel or Ni superalloy substrate of which turbine blades as well as parts of diesel engines are made. In order to obtain better adherence of the sprayed ceramic layer, a transition cover of a Ni alloy enriched in Al or Zr is sprayed onto the substrate first. The liquid oxides on the substrate surface with a metallic transition layer often solidify in a glassy way due to a very fast solidification rate [1]. In the following sublayers of the ceramics, fine crystal phases, columnar crystals and crystal oxides in the form of lamellas and equiaxial grains have been detected [2]. Since the amorphous oxide sublayer is brittle and it undergoes partial crystallisation which brings about strains in the material, an initial annealing of the joint is usually carried out at temperatures from 1600°C do 2400°C in dependence on the layer material.

It is crucial to predict the microstructure and chemical composition of the expected amorphous phases, which has been the objective of the present study in ceramic alloys of composition presented in Table 1.

TABLE

Chemical properties of the investigated alloys

Alloy	Composition	Liquidus temp. [°C]	Eutectic comp. [wt.%]	Eutectic temp. [°C]
Al_2O_3+SiO_2	30 wt.% SiO_2 42 mole fraction SiO_2	1860	22 SiO_2	1840
Al_2O_3+TiO_2	40 wt.% 50 mole fraction TiO_2	1840	40 TiO_2	1840
Al_2O_3+ZrO_2	40 wt.% ZrO_2 40 mole fraction ZrO_2	1900	40 ZrO_2	1900
ZrO_2+Y_2O_3	20 wt.% Y_2O_3 20 mole fraction Y_2O_3	2805	20 Y_2O_3	2380

* INSTITUTE OF METALLURGY AND MATERIALS SCIENCE, POLISH ACADEMY OF SCIENCES, 30-059 KRAKÓW, 25 REYMONTA STR., POLAND

Using general measure of the alloy tendency to amorphisation, the values of e/a, where a_x is a diameter of the alloy addition, were calculated.

Alloy (1)	e/a = 20	e = 15.2	a_{Si} = 0.76 A
Alloy (2)	e/a = 12.6	e =15.2	a_{Ti} = 1.2 A
Alloy (3)	e/a = 10.1	e =15.6	a_{Zr} = 1.54 A
Alloy (4)	e/a = 6.1	e = 9.4	a_Y = 1.54 A

The Tl/Tg criterion (ratio of melting temperature to the amorphisation temperature) could not be applied, because of the lack of reliable data of the amorphisation temperatures. Inoue [3] and Dutkiewicz [4] established that the higher the e/a ratio the easier the amorphisation in metallic alloys. The phenomenon of the increase of susceptibility to amorphisation with the increase of the atom diameter of some metals was explained at least for AgCuCe, AgCuGe, AgCuSb alloys produced with melt spinning method. It was found, that large atoms promoted amorphisation as they obstruct the nucleation of crystallite from the liquid phase. The e/a values were 1.8, 1.84, and 2.44 for Ce, Sb and Ge additions, respectively. The Tl/Tg was 0.63. The problem is more complex in ceramic alloys because of the formation of glassy phases from metal oxides. In this case, sizes of atoms and their ions as well as the size of oxygen atoms have to be dealt with. Assuming the ratio of atom diameter of the alloy addition to that of the metal oxide it seems that the tendency goes the other way round, that is, the tendency to amorphisation increases with the decrease of the atom size of alloy addition.

The most favourable conditions to form the amorphous phase can be obtained in eutectic or semi-eutectic alloys such as alloys 1–3, studied in this research. Apart from these, the fourth alloy was quite far in composition from the eutectic one, but anyway all the selected materials find commercial application and thus they are worth to be studied.

Based on the calculated e/a values it was proposed, that material (1) (Al_2O_3+SiO_2) should become glassy in the easiest way during plasma spraying, while material (4) (ZrO_2+Y_2O_3) should be the most difficult to transform into an amorphous state. The amount of the material transformed could be the measure of the susceptibility to amorphisation.

In order to gain the data on the process of crystallite formation in the amorphous phase, the plasma sprayed samples were annealed according to the following schedule:

alloy (2)	Ta = 1150°C for15 hrs
alloy (3)	Ta = 1350°C for 15 hrs
alloy (4)	Ta = 900°C for 50 hrs.

These conditions were established experimentally as the most suitable to ensure optimal decrease of stresses in the plasma sprayed layers as well as in the sublayer of the glassy phase.

2. Experimental procedure

The plasma spraying of ceramic powders melted in an electric arch in plasma hydrogen and argon atmosphere was carried out in PN-120 plasmothrone in Świerk, Poland according to parameters given in the work of Górski [5]. The ceramics was introduced into the plasmothrone as Al_2O_3, ZrO_2, Y_2O_3, SiO_2 powders at appropriate fractions with grains 10–50 μm in size. It took several milliseconds to reach temperature about 10^4 K, while the cooling rate of the layer obtained on the metallic substrate, was 10^5–10^6 K/s. A Ni-based super-alloy or stainless steel was the substrate, which was first plasma sprayed with a Ni-20 Cr-5 Fe-2 Al to improve the adherence of the ceramic cover. The thicknesses of the ceramic layers obtained were about 200 μm. The joints were annealed at 900 up to 1350°C in order to decrease stresses of the material.

The detailed phase morphology analyses of the ceramic layers were carried out at cross-sections using a transmission microscope (TEM) Philips CM20 TWIN. Thin foils were produced with mechanical polishing using so called Trod device followed by thinning with focused Ga^+ ion beam (FIB) technique in a Quanta 3D thinning instrument. Local analyses of chemical composition were performed using 10 nm wide beam measured as full width at high maximum and energy dispersive X-ray spectrometer (Phoenix EDAX) and EDX HAADF Detector.

The heat effects were recorded during crystallisation of the Al_2O_3+40 wt.% TiO_2 alloys plasma sprayed and annealed at 1150°C for 15 hrs using DSC-TGA microcalorimeter (TA Instruments SDT Q 600).

3. Results and discussion

3.1. Microstructure of the Al_2O_3+30 wt.% SiO_2 ceramics

The TEM microstructure of the ceramic layer of composition Al_2O_3+30 wt.% SiO_2 plasma sprayed on a metallic substrate obtained with the FIB technique is shown in Fig. 1a. It can be seen that the Al_2O_3 – SiO_2 based amorphous phase existed close to the substrate between the transition NiCrFeAl layer visible in right, upper corner of the photograph and etched out particles visible in the left side. A selected area diffraction pattern SAED taken in the centre of the microstructure confirmed its amorphous morphology. The chemical composition analyses (EDX) are shown in Fig. 2a and 2b. Figure 2a shows the Al_2O_3 enrichment in the area marked with a cross, while Fig. 2b presents the area rich in SiO_2 in the lower part of the micrograph. These facts suggested a strong differentiation of the composition in the plasma sprayed ceramic material. Some cristallities in the amorphous phase did not appear.

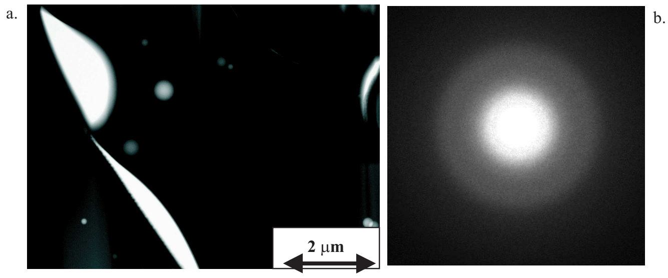

Fig. 1. TEM Microstructure of Al_2O_3-%SiO_2 based amorphous phase, (a); together with corresponding (SAED) (b)

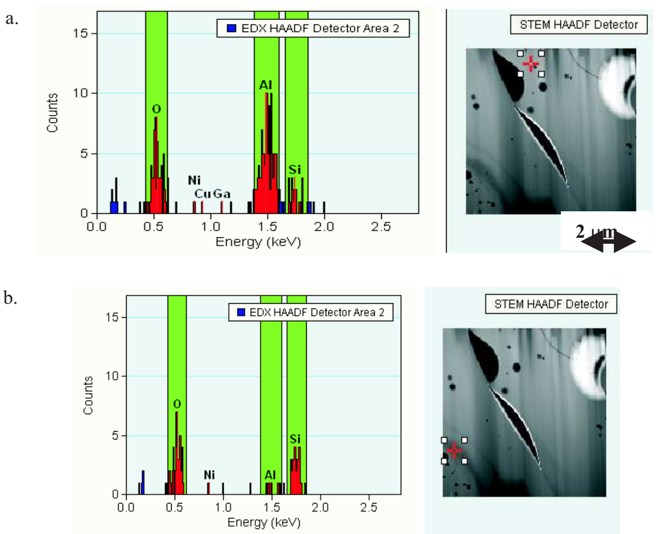

Fig. 2. Chemical compositions of the amorphous phases in the area of the micrograph, enriched in Al_2O_3, (a); enriched in SiO_2, (b)

3.2. Microstructure of the Al_2O_3+40 wt.% TiO_2 ceramics

The TEM microstructure of the plasma sprayed ceramic Al_2O_3+40 wt.% TiO_2 layer close to the metallic substrate is shown in Fig. 3 a, in which the area of the amorphous phase is visible along with big number of nanocrystallites, about 20 nm in size, appeared as a result of annealing at 1150°C for 15 hours. Reflections in SAED in Fig. 3b come from the nanocrystals of the Al_2O_3-α and TiO_2 phases, while the circle from the amorphous phase.

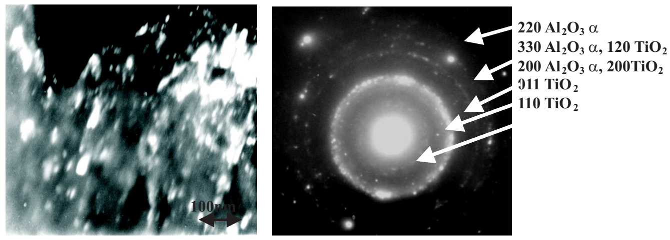

Fig. 3. TEM Microstructure of Al_2O_3-TiO_2 based amorphous phase, (a); with corresponding (SAED), (b) [6]

3.3. Microstructure of the Al_2O_3+40 wt.% ZrO_2 ceramics

The TEM microstructure of the plasma sprayed ceramic Al_2O_3+40 wt.% ZrO_2 layer close to the metallic substrate is shown in Fig. 4a, in which fragments of the Al_2O_3-ZrO_2 based amorphous phase less than 1 μm wide are visible on the metallic transition surface. SAED in Fig. 4b taken from the area marked with arrow shows a circle consisting of reflections corresponding to the amorphous phase.

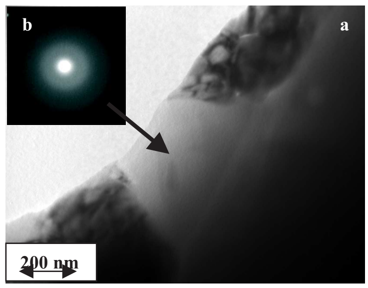

Fig. 4. TEM Microstructure of Al_2O_3-ZrO_2 based amorphous phase observed on a cross-section, (a); together with corresponding (SAED, (b)

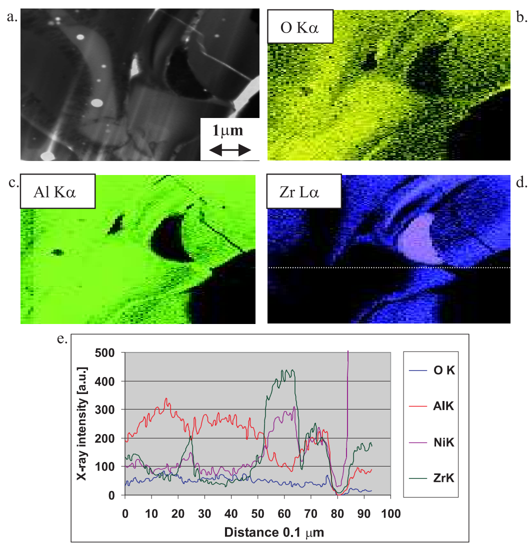

Fig. 5. TEM Microstructure of Al_2O_3-ZrO_2 based amorphous phase close to the substrate observed on cross-section, (a); maps of distribution of elements: O_2, (b): Al, (c), Zr, (d); changes of Zr content along the line marked in d, e.[7]

The TEM microstructure of Al_2O_3-ZrO_2 based amorphous phase observed on cross-section close to the substrate is visible in Fig. 5 a, together with maps of element distributions (Figs. 5 (b-d) and the changes of Zr content along the line marked in d, e.

3.4. Microstructure of the ZrO_2+20 %Y_2O_3 ceramics

The observations of TEM microstructure of the plasma sprayed ceramic ZrO_2+20 wt.% Y_2O_3 layer close to the metallic substrate is shown in Fig. 6, in which the ZrO_2-Y_2O_3 based amorphous phase can be seen. A area in Fig.6a its presence was confirmed by the rings of reflections in the corresponding SAED, in which also reflections from nanocrystalline particles of tetragonal ZrO_2 phase resulted from the annealing of the joint at 900°C for 50 hrs could be observed (Fig. 6c). The SAED taken of the area away from the amorphous phase (marked K) showed reflections from the same particles (Fig. 6b).

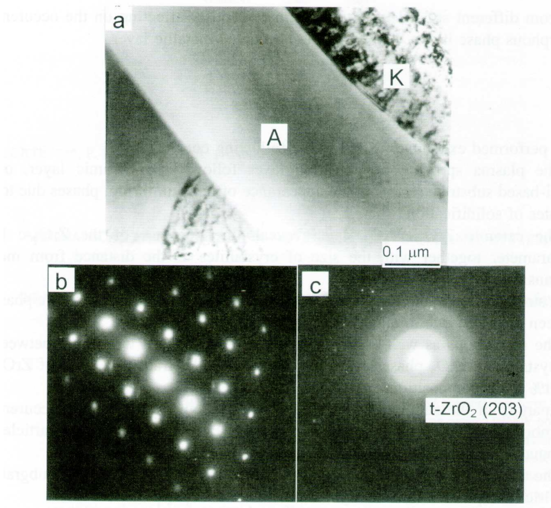

Fig. 6. TEM Microstructure of grain of amorphous phase (A) surrounded by grains containing ZrO_2(t) (203) crystallites marked with K, (a); SAED taken from the area marked by K, (b); SAED taken of the area marked by A (c) [2]

3.5. Measurements of heat effects

The example of heat effect measurements using DSC-TGA instrument during crystallisation of the Al_2O_3+40 wt.% TiO_2 alloy plasma sprayed and annealed at 1150°C for 15 hrs is presented in Fig.7. Temperature of crystallisation has been assessed to be 1233°C, while the temperature of the glass formation could not be determined unambiguously. I may only be suggested to be 1207°C. On the heat effects curve 1285°C was marked as the crystallisation temperature of Al_2O_3-α (corundum), and 1435°C for the crystallisation of Al_2TiO_5.

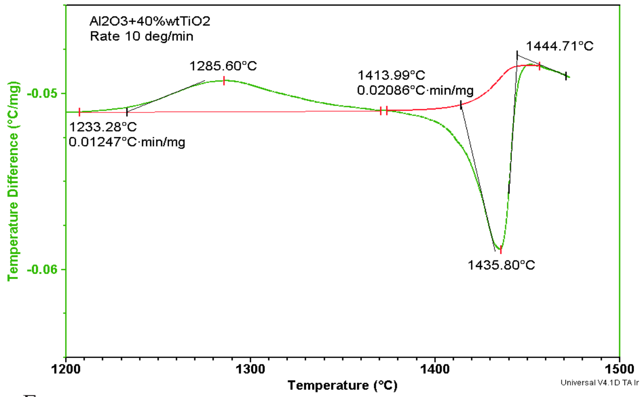

Exo up

Fig. 7. DTA curve of heat output during continuous heating of the Al_2O_3-TiO_2 alloy up to 1500°C

The presented results of the study of microstructure, crystallography and chemical (EDX) composition using TEM were generally in accordance with the calculated tendencies to amorphisation of the analysed ceramic materials, which were plasma sprayed on an air cooled (100°C) substrate of Ni super alloy or alloyed steel.

It was established, that the sublayer of amorphous phase prevailed in the structure appeared at plasma spraying of material (1) Al_2O_3+30wt.%SiO_2, which resulted from the influence of the Si atoms of small diameter 0.76A and high e/a ratio=20. Thus, it seemed, that the small diameter of the Si atoms and high value of e/a ensured the high tendency to amorphisation. The differentiation of the composition of the amorphous phase as regards the amount of the SiO_2, showed that there was more Al_2O_3 than SiO_2 in the vicinity of the substrate.

In material (2) of Al_2O_3+40wt.% TiO_2 composition, the amorphous sublayer was quite wide (about 5μm, which suggested its high susceptibility to amorphisation at e/a parameter equal to12.6 and the Ti atom size equal to 1.2 A. The annealing of the joint at 1150°C for 15 hrs brought about the appearance of great number of Al_2O_3-α and TiO_2 nanocrystallites on the expense of the amorphous phase. This indicated that the temperature of its transition in crystalline form is lower than 1150°C.

In material (3) of Al_2O_3+40%ZrO_2 composition, the amorphous sublayer was relatively narrow (about 1 μm), e/a parameter equal to 10.1 and Zr atom diameter was 1.54 A, which was twice as big as that for Si contained in material (1). During annealing at 1350°C for 15 hrs nanocrystallites did not appeared. Therefore the transformation temperature must have been higher.

Material (4) of ZrO_2+20%Y_2O_3 composition, the amorphous sublayer was also narrow (1-2 μm,) which could result from lower value of parameter e/a=6.1 and atomic diameter of Zr a=1.54 A. The composition of the amorphous layer close to the substrate was inhomogeneous; enrichments in ZrO_2 or even its tetragonal particles were observed. The annealing at 900°C for 50 hrs induced the formation of nanocrystalline phases in the amorphous area probably as an effect of prolonged annealing.

4. Conclusions

Based on the presented results and their discussion the following conclusions have been formulated:

- The tendency to amorphisation analysed through microstructure investigation of plasma sprayed Al_2O_3 and ZrO_2 materials with TiO_2 and Y_2O_3 additions seemed to depend on the value of e/a parameter as well as the size of atom diameter of the alloy addition. The susceptibility to amorphisation increased with higher e/a parameter and the smaller atom size. Such a relation was confirmed for all four alloys examined in such a way, that the Al_2O_3+30%SiO_2 with e/a=20 was the most prone to amorphisation. The Al_2O_3+40%TiO_2 alloy with e/a=12.6 was less prone and even less susceptible was the Al_2O_3+40%ZrO_2 with e/a=10.1. The lowest tendency for amorphisation was observed in the ZrO_2+20%Y_2O_3 with e/a=6.1.
- The diameter of silicon atoms was the smallest (a=0.76 A) at the greatest tendency of the Al_2O_3+30%SiO_2 alloy to amorphisation, while that of itrium the biggest (1.54 A), which meant the least susceptibility to amorphisation of the alloy ZrO_2+20%Y_2O_3. The diameter of oxygen (2.92 A) was not considered as its influence was the same for all the alloys.
- Crystallisation of the amorphous phase in the investigated alloys seemed to depend on temperature and time of annealing. Prolonged annealing of the alloy (4) ZrO_2+20%Y_2O_3, ensured the partial transformation of the amorphous phase into a crystalline one.
- Partial crystallisation of the amorphous phase was observed in alloys (2 with Ti) and (4 with Y), which had the highest values of atomic diameters (Ti and Y). It seemed that the higher atom size of the alloy addition and smaller tendency to amorphisation the easier is the reverse transition from amorphous into crystalline phase.

Received: 21 May 2007.

REFERENCES

[1] A. Pawłowski, T. Czeppe, L. Górski, W. Baliga, Structure Changes of the Plasma Sprayed Al_2O_3-TiO_2 Layer and its Adhesion to the Substrate after Thermal Shocks, Archives of Metallurgy and Materials **50**, 3, 719 (2005).

[2] A. Pawłowski, T. Czeppe, L. Górski, The Phase Structure of Metallic and Ceramic Plasma Sprayed Protective Coatings, Archives of Metallurgy **47**, 4, 399-408 (2002).

[3] A. Inoue, I. Part, T. Massuanmoto, Formation of Amorphous CuAgCe Alloys by Rapid Solidification and Transformed Thermal and Mechanical Properties, Mater. Trans. JIM **35**, 227 (1994).

[4] J. Dutkiewicz, T. Massalski, Research for Metallic Glasses of Eutectic Crystallisations in the AgCuCe, AgCuSb and AgCuGe Systems. Metall.Trans. **2A**, 773 (1981).

[5] L. Górski, Phase transformations in plasma sprayed and annealed Al_2O_3 ceramic materials, in Polish. Przemiany fazowe w materiałach ceramicznych na bazie Al_2O_3 w warunkach natryskiwania plazmowego i wygrzewania stacjonarnego, Inż. Mater. **1**, 16 (1994).

[6] T. Czeppe, A. Pawłowski, W. Baliga, L. Górski, Analytical electron microscopy study of Plasma sprayed layers solidified on the metallic substrate. Archives of Materials Science **26**, 1, 103-109 (2005).

[7] A. Pawłowski, J. Morgiel, L. Górski, Structure of the Plasma Sprayed Al_2O_3-ZrO_2 Ceramic Layer onto Metallic Substrate, Polska Metalurgia **2002-2006**, 803-808 (2006).